RNA Folding

DOI: 10.1002/anie.201200526

Single-Molecule FRET Reveals the Folding Dynamics of the Human Telomerase RNA Pseudoknot Domain**

*Martin Hengesbach, Nak-Kyoon Kim, Juli Feigon, and Michael D. Stone**

Telomerase-catalyzed synthesis of telomere DNA provides the foundation for the DNA–protein structures known as telomeres. Telomeres are required to evade DNA processing that may result in nucleolytic degradation and fusion of linear chromosomes. Human telomeres are maintained by a complex of human telomerase reverse transcriptase (hTERT), human telomerase RNA (hTR), and several additional proteins.[1] hTR provides the template sequence for hTERT during a novel reverse transcription reaction that produces short telomere DNA repeat sequences.[2] Additionally, hTR provides a flexible scaffold for the assembly and function of telomerase-associated proteins[3] and has recently been suggested to contribute to hTERT catalysis.[4] Many pathogenic mutations have been mapped to hTR;[5] however the precise mechanisms of how these mutations cause disease remain unclear.

In vitro reconstitution of hTR with hTERT into a catalytically active enzyme requires two separable RNA domains, containing several conserved structural motifs, including an RNA pseudoknot (PK) fold.[5–10] In PK structures, nucleotides in a hairpin loop make base pairing contacts with nucleotides upstream or downstream of the hairpin. NMR spectroscopy studies of the structures of wild-type and mutant minimal (truncated) hTR PK constructs have revealed tertiary interactions in the folded pseudoknot that form a conserved triple helix, as well as a partially folded hairpin.[10–15] Single-molecule experiments have used mechanical force to probe the folding/unfolding of a minimal PK construct[11] and a modified two-color coincidence detection assay to examine the distribution of RNA conformations for a larger hTR PK domain in solution.[16] Owing to the large size of the native hTR PK domain, analyses of its folding properties have to date been largely limited to truncated variants of the natural RNA sequence. To circumvent this challenge, we use a single-molecule Förster resonance energy transfer (smFRET) assay[17] (which measures the efficiency of excitation energy transfer between a donor Cy3 dye and acceptor Cy5 dye) to analyze the folding and dynamics of the minimal hTR PK and a larger functional hTR PK domain. Using a combination of smFRET and high-resolution NMR spectroscopy measurements, we have determined the contribution of Mg^{2+} ions, RNA triplex formation, and the native hTR sequence to PK domain folding and stability.

We initially designed a minimal hTR PK construct ($minPK_{WT}$) similar to the hTR fragments used in previous NMR spectroscopy studies (Figure 1a).[13] FRET-labeled $minPK_{WT}$ was annealed to a biotinylated DNA handle oligonucleotide, immobilized on a streptavidin-coated microscope slide, and imaged using prism-type total internal

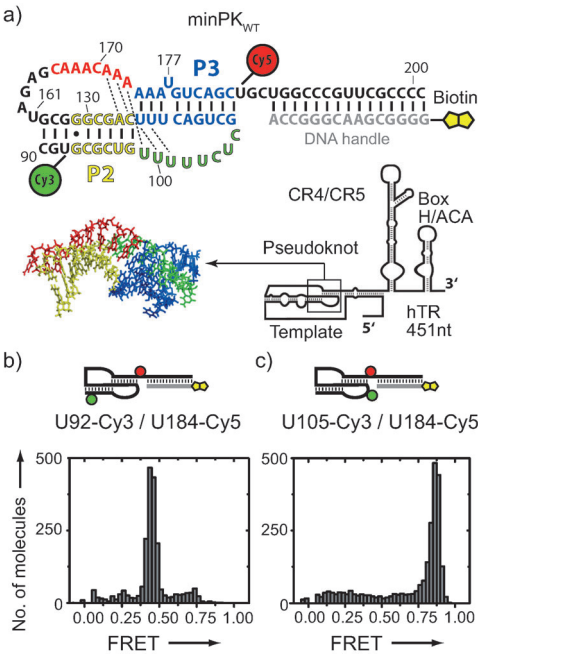

Figure 1. Design and validation of a minimal hTR pseudoknot smFRET construct. a) Schematic diagram of smFRET $minPK_{WT}$ construct. Nucleotide numbering corresponds to the native full-length hTR sequence. b) FRET efficiency distribution for $minPK_{WT}$ (U92-Cy3/U184-Cy5). c) FRET efficiency distribution for $minPK_{WT}$ (U105-Cy3/U184-Cy5). Data in (b) and (c) were acquired in the presence of telomerase imaging buffer (see Supporting Information) containing 1 mM Mg^{2+}.

[*] M. Hengesbach, Prof. M. D. Stone
Department of Chemistry and Biochemistry, Center for Molecular Biology of RNA, University of California Santa Cruz
Santa Cruz, CA 95064 (USA)
E-mail: mstone@chemistry.ucsc.edu
Homepage: http://stone.chemistry.ucsc.edu
Prof. J. Feigon
Department of Chemistry and Biochemistry
University of California Los Angeles, Los Angeles, CA 90095 (USA)
N.-K. Kim
Advanced Analysis Center, Korea Institue of Science and Technology, Seoul (Republic of Korea)

[**] We thank Prof. Kathleen Collins for the gift of FLAG-tagged hTERT plasmid and Prof. Julian Chen for the gift of the hTR expression plasmid. This work was financially supported by the following grants: NIH GM095850 to M.D.S. and NIH GM048123 to J.F. M.H. is supported by a German Research Foundation fellowship (DFG HE6181/1-1). FRET = Förster resonance energy transfer.

Supporting information for this article (experimental details) is available on the WWW under http://dx.doi.org/10.1002/anie.201200526.

reflection fluorescence (TIRF) microscopy. The $minPK_{WT}$ with U92-Cy3 and U184-Cy5 modifications yielded an RNA population with a FRET efficiency centered at 0.45 (Figure 1b), a value consistent with the distance between these two U residues in the analogous NMR structure (Supporting Information, Figure S1).[13] We then altered the position of the donor Cy3 dye to U105 (closer to the U184-Cy5), which shifts the FRET efficiency distribution to a higher value (corresponding to a shorter distance) as predicted for the folded $minPK_{WT}$ (FRET efficiency = 0.87, Figure 1c). Taken together with additional control experiments (Supporting Information, Figure S2), these results demonstrate that the smFRET system accurately reports the folding of $minPK_{WT}$.

Next, we analyzed the impact of Mg^{2+} ions on $minPK_{WT}$ folding and dynamics. The FRET efficiency distribution in the absence of Mg^{2+} ions centered on FRET efficiency = 0.44. However, close inspection of the time traces revealed rapid structural changes in the absence of Mg^{2+} ions between the folded PK and an alternative higher FRET efficiency conformation in the majority (56%, $n = 312$) of molecules (Figure 2b and Figure S3). These structural dynamics are consistent with a transient sampling of the reported P2 hairpin structure.[13] In contrast, addition of 1 mM Mg^{2+} ions suppressed these structural dynamics completely at the time resolution of our measurements (Figure 2a, right panel and Figure S4). We next analyzed the structural impact of the pathogenic GC(107–108)AG mutation that is genetically linked to the blood disorder Dyskeratosis Congenita (DKC).[19] In the absence of Mg^{2+} ions, the minimal hTR_{DKC} PK domain ($minPK_{DKC}$) yielded a FRET efficiency distribution indicative of the folded PK (FRET efficiency = 0.50) as well as multiple alternative conformations (FRET = 0.62 and 0.75, Figure 2c, left panel), in accordance with the significant destabilization of the native PK fold expected for these mutations.[13–15] Addition of a compensatory GA(182–183)CU mutation, which rescues the Watson–Crick base pairing affected by the DKC mutant, largely recovered the FRET efficiency of the native PK fold in the presence or absence of Mg^{2+} (Supporting Information, Figure S5). Surprisingly, addition of 1 mM Mg^{2+} ions completely suppressed the DKC mutant folding defect (Figure 2c, right panel). Analysis of single-molecule trajectories in the absence of Mg^{2+} ions revealed very slow structural dynamics for $minPK_{DKC}$ between the PK fold and alternative conformations in the majority (64%, $n = 214$) of molecules (Figure 2d and Figure S3). Importantly, the occurrence of alternative conformations in our experiments was not dependent on the presence or absence of Mg^{2+} ions during the initial folding of the RNA (Supporting Information, Figure S6).

The *K. lactis* PK has been reported to require Mg^{2+} ions for compaction into a conserved RNA triplex structure,[20] similar to DNA triplexes.[21] However, triplex formation in the hTR PK cannot require Mg^{2+} ions, because the NMR structure that identified the tertiary interactions was solved in the absence of Mg^{2+} ions.[13] This structure revealed an H-type pseudoknot with P2 and P3 stems stabilized by a central triplex consisting of five base triples flanking the A173–U99 junction Hoogsteen base pair (Figure 1a).[13] Our smFRET approach does not permit us to differentiate between a PK

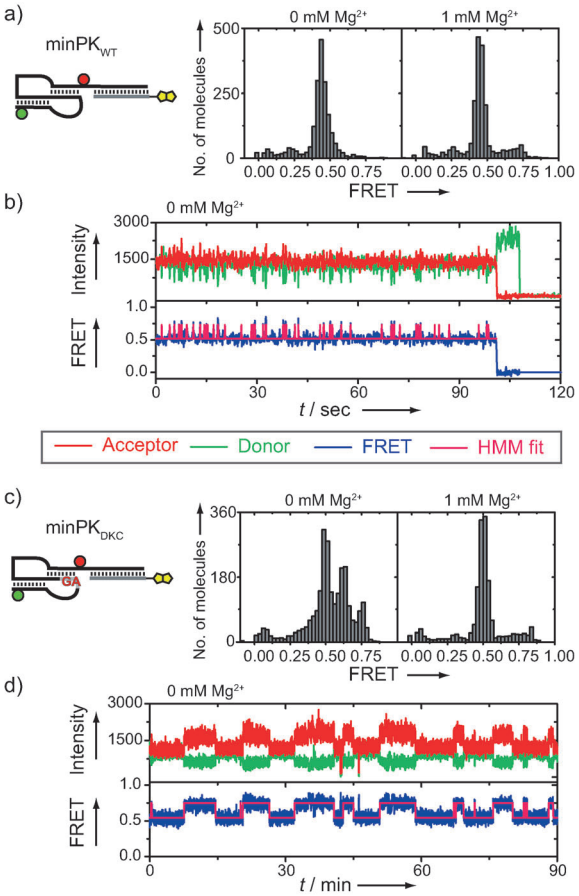

Figure 2. Mg^{2+} ion-dependent folding and dynamics of minimal hTR pseudoknot domain. a) FRET efficiency distribution for $minPK_{WT}$ in the absence (left panel) or presence (right panel) of 1 mM Mg^{2+} ions. b) Representative single-molecule FRET trace of $minPK_{WT}$ in the absence of Mg^{2+} ions. The abrupt loss of signal intensity at the end of the trace is due to photobleaching of the dye. Hidden Markov Modeling (HMM)[18] of the FRET trajectories yielded idealized-state traces (magenta), which were used to calculate transition rates between observed FRET states (Supporting Information, Figure S3). c) FRET efficiency distribution for $minPK_{DKC}$ in the absence (left panel) or presence (right panel) of 1 mM Mg^{2+} ions. d) Representative single-molecule trace of $minPK_{DKC}$ in the absence of Mg^{2+} ions.

structure comprised of only the P2 and P3 stems, and the further stabilized PK structure possessing additional triplex forming tertiary contacts identified in the NMR structure. Therefore, we investigated the folding of a PK with UU(99–100)CC substitutions ($minPK_{C99C100}$), which disrupt the tertiary interactions by abolishing the junction Hoogsteen base pair and one base triple but would still in principle allow the P2 and P3 stems to form.[14,22]

In the absence of Mg^{2+} ions, FRET efficiency distributions generated with $minPK_{C99C100}$ centered on a value consistent with a folded PK (FRET efficiency = 0.48; Figure 3a, left panel). NMR spectroscopy experiments with a similar construct containing the UU(99–100)CC mutant in the absence of Mg^{2+} ions indicated that the P2 and P3 stems are partially formed, but the tertiary triplex interactions are disrupted (Supporting Information, Figure S7). In striking contrast, FRET efficiency distributions of $minPK_{C99C100}$ in the presence

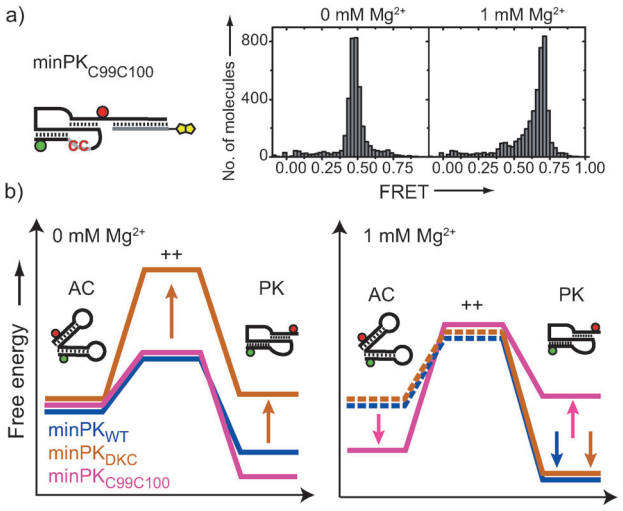

Figure 3. a) FRET efficiency distribution for minPK$_{C99C100}$ in the absence (left panel) or presence (right panel) of 1 mM Mg^{2+} ions. b) Schematic energy diagrams of the Mg^{2+}-dependent folding of a minimal hTR pseudoknot domain (see text for details). ++ = transition state, dashed lines = states not directly detected in our experiments.

A powerful attribute of smFRET is the ability to analyze RNA folding within the larger native hTR PK domain. Using DNA-splinted RNA ligation, we generated a smFRET construct comprising hTR nucleotides 39–201 with U92-Cy3 and U184-Cy5 modifications (Figure 4a and Figure S10). This nearly full-length hTR PK WT domain (fullPK$_{WT}$) can be reconstituted with the CR4/CR5 RNA domain and hTERT protein in rabbit reticulocyte lysates to produce catalytically active telomerase enzyme.[23] When compared to an in vitro transcribed fullPK$_{WT}$, the smFRET fullPK$_{WT}$ supported approximately 60% of wild-type levels of catalytic activity and showed a slight reduction in repeat addition processivity (Supporting Information, Figure S11).

In the absence of Mg^{2+} ions, we observed a dominant misfolded population of RNA molecules centered on FRET efficiency = 0.1 and no detectable folding of fullPK$_{WT}$, as evidenced by the absence of a population centered at a FRET efficiency of about 0.5 (Figure 4b). This result contrasts with our observations of minPK$_{WT}$ folding in the absence of Mg^{2+} ions (Figure 2a) and reveals that the folding requirements for fullPK$_{WT}$ are more stringent, which is expected for a larger RNA. Interestingly, in a near-physiological buffer (1 mM Mg^{2+}) around 50% of the fullPK$_{WT}$ molecules fold into a conformation consistent with a folded PK domain (FRET efficiency = 0.48; Figure 4b and Figure S12). To further validate the assignment of the 0.48 FRET efficiency state as the folded fullPK$_{WT}$, we measured the FRET efficiency distribution for a fullPK$_{WT}$ construct containing the GC-(107–108)AG DKC mutation (fullPK$_{DKC}$). Interestingly, whereas small amounts of Mg^{2+} ions were sufficient to

of 1 mM Mg^{2+} ions shifted to a substantially higher FRET value (FRET efficiency = 0.69; Figure 3a, right panel, and Figure S8), indicative of an alternative RNA conformation.

Taken together, these experiments reveal that both minPK$_{WT}$ and minPK$_{DKC}$ exhibit structural dynamics in the absence of Mg^{2+} ions, albeit with markedly different kinetics (Figure 3b, left panel): minPK$_{WT}$ is predominantly in the PK state, but transiently samples an alternative conformation (AC). Note, the structure drawn for AC is not intended to represent the actual conformation but is based upon secondary structure calculations (Supporting Information, Figure S9). In contrast, minPK$_{DKC}$ shows a significantly destabilized PK fold and exhibits structural interconversion with AC on a much slower time scale, as indicated by a significantly higher energy transition state. The stability of the PK fold for minPK$_{C99C100}$ is very similar to minPK$_{WT}$ (Supporting Information, Figure S8). In the presence of 1 mM Mg^{2+} ions (Figure 3b, right panel), both minPK$_{WT}$ and minPK$_{DKC}$ are stabilized in the PK fold. In contrast, minPK$_{C99C100}$ is stabilized in the AC. Moreover, near-physiological Mg^{2+} ion levels stabilize both minPK$_{WT}$ and minPK$_{DKC}$ folding into the PK structure, raising the question of how the pathogenic DKC mutation disrupts telomerase activity in vivo? Finally, experiments with minPK$_{C99C100}$ demonstrate that destabilization of the RNA triplex increases the probability of the minimal PK domain misfolding under physiological conditions.

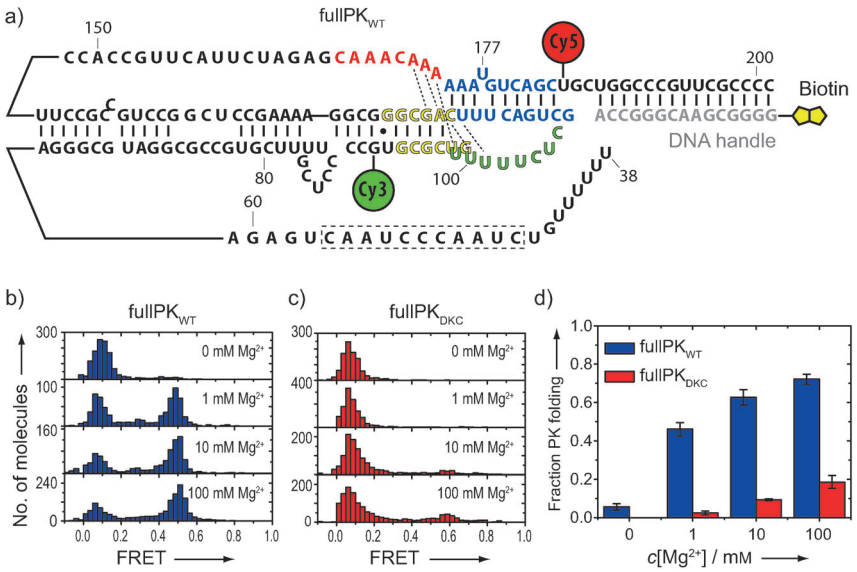

Figure 4. Mg^{2+} ion-dependent folding of the nearly full-length hTR PK domain. a) Schematic diagram of the fullPK$_{WT}$ smFRET construct sequence with FRET dyes and DNA handle oligonucleotide attached as described for the minPK$_{WT}$. b) FRET efficiency distributions for fullPK$_{WT}$ as a function of [Mg^{2+}]. c) FRET efficiency distributions for the fullPK$_{DKC}$ as a function of [Mg^{2+}]. d) Quantification of pseudoknot formation at varying Mg^{2+} ion concentrations. The fraction of fullPK$_{WT}$ (blue) or fullPK$_{DKC}$ (red) exhibiting PK folding. Error bars represent the standard deviation of experiments done in triplicate.

rescue the folding defects of $minPK_{DKC}$, we detected no PK domain folding for $fullPK_{DKC}$ in the near physiological buffer (1 mM Mg^{2+}; Figure 4c). Moreover, whereas the fraction of folded $fullPK_{WT}$ molecules continued to increase at elevated Mg^{2+} ion concentrations (Figure 4d), only 20% of $fullPK_{DKC}$ folded into a PK conformation at the highest Mg^{2+} ion concentration tested (100 mM Mg^{2+}). Taken together, these results support the assignment of the 0.48 FRET efficiency state to the native PK fold and reveal that within the context of the $fullPK_{DKC}$, physiological levels of Mg^{2+} ions are not sufficient to suppress the folding defects incurred by the GC(107–108)AG DKC mutation, suggesting that the pathogenic phenotype observed for this mutation is due to an RNA folding defect (Supporting Information, Figure S13).

In summary, our results demonstrate the hTR PK domain has the intrinsic ability to form alternative conformations distinct from the native pseudoknot fold. Experiments with the minPK suggest a model for PK domain folding, wherein the P2 and P3 stems of the hTR PK form in a Mg^{2+} ion-independent manner together with a Mg^{2+} ion-induced stabilization of tertiary triplex interactions. The unique capability of smFRET to probe fullPK folding highlights the importance of Mg^{2+} ions in stabilizing the native PK fold. Moreover, the inability of the $fullPK_{DKC}$ construct to fold under near-physiological conditions provides unique insights into the structural basis of this pathogenic RNA mutation. Recent experiments analyzing the folding of the RNA pseudoknot in *Tetrahymena thermophila* telomerase RNA demonstrated a requirement for telomerase proteins to achieve the native pseudoknot fold.[24] The propensity of the hTR PK domain to fold under the near-physiological conditions reported herein highlights an important difference in the intrinsic stabilities of the human and *Tetrahymena* RNA pseudoknot domains.[16] Finally, the method established in this study provides an essential experimental framework for future investigation of hTR PK structure and dynamics within the functional telomerase ribonucleoprotein complex.

Received: January 18, 2012
Revised: March 10, 2012
Published online: April 27, 2012

Keywords: FRET · NMR spectroscopy · RNA structures · single-molecule studies

[1] K. Collins, *Nat. Rev. Mol. Cell Biol.* **2006**, *7*, 484.
[2] C. W. Greider, E. H. Blackburn, *Nature* **1989**, *337*, 331.
[3] E. D. Egan, K. Collins, *Mol. Cell. Biol.* **2010**, *30*, 2775.
[4] F. Qiao, T. R. Cech, *Nat. Struct. Mol. Biol.* **2008**, *15*, 634.
[5] C. A. Theimer, J. Feigon, *Curr. Opin. Struct. Biol.* **2006**, *16*, 307.
[6] J. L. Chen, M. A. Blasco, C. W. Greider, *Cell* **2000**, *100*, 503.
[7] J. R. Mitchell, K. Collins, *Mol. Cell* **2000**, *6*, 361.
[8] V. M. Tesmer, L. P. Ford, S. E. Holt, B. C. Frank, X. Yi, D. L. Aisner, M. Ouellette, J. W. Shay, W. E. Wright, *Mol. Cell Biol.* **1999**, *19*, 6207.
[9] Q. Zhang, N. K. Kim, J. Feigon, *Proc. Natl. Acad. Sci. USA* **2011**, *108*, 20325.
[10] Q. Zhang, N. K. Kim, R. D. Peterson, Z. Wang, J. Feigon, *Proc. Natl. Acad. Sci. USA* **2010**, *107*, 18761.
[11] G. Chen, J. D. Wen, I. Tinoco, Jr., *RNA* **2007**, *13*, 2175.
[12] L. R. Comolli, I. Smirnov, L. Xu, E. H. Blackburn, T. L. James, *Proc. Natl. Acad. Sci. USA* **2002**, *99*, 16998.
[13] N. K. Kim, Q. Zhang, J. Zhou, C. A. Theimer, R. D. Peterson, J. Feigon, *J. Mol. Biol.* **2008**, *384*, 1249.
[14] C. A. Theimer, C. A. Blois, J. Feigon, *Mol. Cell* **2005**, *17*, 671.
[15] C. A. Theimer, L. D. Finger, L. Trantirek, J. Feigon, *Proc. Natl. Acad. Sci. USA* **2003**, *100*, 449.
[16] J. A. Yeoman, A. Orte, B. Ashbridge, D. Klenerman, S. Balasubramanian, *J. Am. Chem. Soc.* **2010**, *132*, 2852.
[17] M. D. Stone, M. Mihalusova, C. M. O'Connor, R. Prathapam, K. Collins, X. Zhuang, *Nature* **2007**, *446*, 458.
[18] S. A. McKinney, C. Joo, T. Ha, *Biophys. J.* **2006**, *91*, 1941.
[19] T. Vulliamy, A. Marrone, F. Goldman, A. Dearlove, M. Bessler, P. J. Mason, I. Dokal, *Nature* **2001**, *413*, 432.
[20] K. Shefer, Y. Brown, V. Gorkovoy, T. Nussbaum, N. B. Ulyanov, Y. Tzfati, *Mol. Cell. Biol.* **2007**, *27*, 2130.
[21] M. D. Frank-Kamenetskii, S. M. Mirkin, *Annu. Rev. Biochem.* **1995**, *64*, 65.
[22] J. L. Chen, C. W. Greider, *Proc. Natl. Acad. Sci. USA* **2005**, *102*, 8080.
[23] T. L. Beattie, W. Zhou, M. O. Robinson, L. Harrington, *Curr. Biol.* **1998**, *8*, 177.
[24] M. Mihalusova, J. Y. Wu, X. Zhuang, *Proc. Natl. Acad. Sci. USA* **2011**, *108*, 20339.

